ATION PAGE

Form Approved
OBM No. 0704-0188

Public reporting burden for this collection of information is estimated to average 1 hour per response, including the time for reviewing instructions, searching existing data sources, gathering and maintaining the data needed, and completing and reviewing the collection of information. Send comments regarding this burden or any other aspect of this collection of information, including suggestions for reducing this burden, to Washington Headquarters Services, Directorate for information Operations and Reports, 1215 Jefferson Davis Highway, Suite 1204, Arlington, VA 22202-4302, and to the Office of Management and Budget, Paperwork Reduction Project (0704-0188), Washington, DC 20503.

1. Agency Use Only *(Leave blank).*	2. Report Date.	3. Report Type and Dates Covered.
	June 1993	Final - Proceedings

4. Title and Subtitle.
Surface forward-scattered acoustic measurements and analysis

5. Funding Numbers.
Program Element No. 0602435N
Project No.
Task No. ONT/RL3B/RO35P03
Accession No.
Work Unit No. 5715253A4

6. Author(s).
E. J. Yoerger, M. Wilson, and S. T. McDaniel*

7. Performing Organization Name(s) and Address(es).
Naval Research Laboratory
Ocean Acoustics Branch
Stennis Space Center, MS 39529-5004

8. Performing Organization Report Number.
NRL/PP/7174--93-0034

9. Sponsoring/Monitoring Agency Name(s) and Address(es).
Naval Research Laboratory
Acoustics Division
Washington, DC 20375

10. Sponsoring/Monitoring Agency Report Number.
NRL/PP/7174--93-0034

11. Supplementary Notes.
Published in Undersea Defence Technology.
*State College, PA

12a. Distribution/Availability Statement.
Approved for public release; distribution is unlimited.

12b. Distribution Code.

13. Abstract *(Maximum 200 words).*

A shallow water, high-frequency acoustic experiment was conducted off the coast of Panama City Florida during August 1991. Acoustic measurements of surface forward scattering, surface reverberation, and direct path intensities were made utilizing two (2) large stationary towers resting on the seafloor. Each tower was equipped with horizontal and vertical receiving arrays, while the two (2) sources were located on only one of the towers. The water bottom was 30 m deep and covered with a fine, rippled sand. The range of acoustic frequencies varied from 20 kHz to 180 kHz. Concurrent environmental measurements including wave heights, sound velocity profiles, and sample cores were made. This paper reports on the surface forward-scattered measurements made at 24 kHz.

14. Subject Terms.
Underwater acoustics, high frequency, electro-optics, geomagnetic, geoelectric, backscattering, mine countermeasures, high resolution imaging, sediment sound transmission

15. Number of Pages.
3

16. Price Code.

17. Security Classification of Report.	18. Security Classification of This Page.	19. Security Classification of Abstract.	20. Limitation of Abstract.
Unclassified	Unclassified	Unclassified	SAR

NSN 7540-01-280-5500

Standard Form 298 (Rev. 2-89)
Prescribed by ANSI Std. Z39-18
298-102

UDT

1993

SP8

PALAIS DES FESTIVALS ET DES CONGRES CANNES, FRANCE 15 - 17 JUNE 1993

Reed Exhibition Companies (UK)

Surface forward-scattered acoustic measurements and analysis

E.J. Yoerger, M. Wilson

Naval Research Laboratory/Stennis Space Center
Code 7174 Stennis Space Center, Mississippi, USA

S.T. McDaniel

The Pennsylvania State University Graduate Program in Acoustics State College, PA.

Abstract

A shallow water, high-frequency acoustic experiment was conducted off the coast of Panama City, Florida during August 1991. Acoustic measurements of surface forward scattering, surface reverberation, and direct path intensities were made utilizing two (2) large stationary towers resting on the seafloor. Each tower was equipped with horizontal and vertical receiving arrays, while the two (2) sources were located on only one of the towers. The water bottom was 30 m deep and covered with a fine, rippled sand. The range of acoustic frequencies varied from 20 kHz to 180 kHz. Concurrent environmental measurements including wave heights, sound velocity profiles, and sample cores were made. This paper reports on the surface forward-scattered measurements made at 25 kHz.

Introduction

This experiment was designed to explore shallow-water acoustic boundary interactions as well as direct-path measurements. However, only the forward-scattered surface measurements are discussed here. It is well known from signal processing and communications theory that adaptive beam forming techniques perform well utilizing coherent processes. Environmental effects disrupt this coherent process such that coherence studies may be used as a measure of this disturbance.

The first section of this paper discusses the experimental design. Such aspects as experimental geometry and layout, environmental measurements, and operating characteristics are detailed. The second section reviews the results of the data analysis. The 25 kHz measurements are discussed and time-domain coherence functions are analyzed. Finally, the conclusions discuss the salient features of this analysis.

Experimental Design

The experimental arrangement for the high-frequency acoustics experiment conducted off the coast of Panama City, Florida in August 1991 is shown in Figure 1. The equipment was deployed in a water depth of 30 m (99 ft) with a flat bottom. The distance between the transmit and receive towers was 90 m (293 ft) with the transmit tower being 2.1 m (7 ft) off the bottom and the receiver tower 7.6 m (25 ft) off the bottom.

The acoustic signals transmitted were 1 ms CW pulses at a frequency of 25 kHz. These pulses were transmitted in groups of 100 with each group representing a different grazing angle. These angles varied from +20 degrees to -20 degrees with plus (+) being towards the surface. The pulses were separated by 1 second between transmissions. The signals were received on an 8-element horizontal and vertical array. The hydrophones for the vertical array were numbered 61 through 68 from bottom to top. The smallest element spacing for this array was 5.08 cm (2 in or 1.18 lambda spacing at 25 kHz). The frequencies transmitted were 20, 25, 40, 60, 90, 110, 130, 150, and 180 kHz. The main lobes of the beam patterns for the circular piston transducers varied from approximately 6 degrees at 20 kHz to 0.5 degrees at 90 kHz at the 3 dB down point.

In order to insure high-quality data analysis, several environmental parameters were monitored during data collection. Measurements of these parameters included CTD casts (sound velocity profiles), wave rider buoy data (power spectrum and wave height distribution), and bottom and mid-depth current meter data. The data recording for this analysis occurred between 0800 and 2300 on August 23. During this time the significant wave height varied from 0.6166 m to 1.4046 m. Downcast and upcast CTD data were collected at 0823 and 1901 on this day.

Data Analysis

The time series data collected on each hydrophone of the array were basebanded and quadrature sampled. The resulting complex time series was used in the data analysis with the time interval between samples being 0.1 ms. Using ray trace model results to match the data, various events are identified on the complex series. Figure 2 shows the important events from this time series. These events include the direct (D), bottom (BB), surface (SB1), and the surface-bottom (SB2) arrivals. Our analysis is concerned only with the surface arrival, which is preceded by the direct and bottom arrival. The surface scattered events occur between 60.0 and 70.0 ms.

Data collection for forward-scattered measurements were made during the time period from 1700 to 2200. The nine 100-ping groups were labeled Run 19 through Run 27. In analyzing each run, a time-domain approach to compute an estimate of the coherence ($\hat{\gamma}(t)$) is used and shown in Equation (1).

$$\hat{\gamma}(t) = \frac{\langle Z_n(t) Z_m^*(t) \rangle}{\sqrt{\langle |Z_n(t)|^2 \rangle \langle |Z_m(t)|^2 \rangle}} \qquad (1)$$

The advantage of a time-domain representation is to more effectively isolate that part of the scattered signal which has interacted only once with the sea surface. This formulation is equivalent to forming the normalized crosscovariance (NCC) function of the complex time series for a pair of hydrophones (n,m) at zero time lag. A typical example of a time covariance function is shown in Figure 3. This plot shows 3 covariance functions from Run 20 with hydrophone 66 as the reference hydrophone. This plot encompasses only the time of interest i.e., the SB1 arrival. One clearly sees the degradation in coherence as one proceeds away from the reference location.

Considering each NCC function for all pairs of hydrophones with respect to a common reference phone yields the spatial coherence across the array. Only the vertical coherence is studied here. Examples of the vertical spatial coherence function for different sea-states are shown in Figure 4. The Run 19 and 20 measurements were made at 1732 and 1750, respectively. The significant wave heights were assumed to build continuously between the 1328 time measurement of 0.7998 m and the 2043 time measurement of 1.1825 m. Hydrophone 66 is used as the reference phone and corresponds to zero receiver separation. Hydrophones below the reference are represented by negative (-) receiver separation and those above it by positive (+) separation. It is clear from the plot that the coherence function deteriorates more quickly with receiver separation for Run 20 than Run 19. This is directly attributable to the rougher sea surface and is further substantiated by later data runs (Run 25, unavailable for publication deadline) .

The results for a similar experiment were published by Dahl and McConnell (1). Their experimental design was comparable to this experiment with the exception of a greater distance between towers. Their results at 30 kHz and rms wave-height of 0.2 m and that of this experiment at 25 kHz and 0.236 wave-height were compared. The comparison showed that the rate of decay for the vertical coherence was significantly faster for the Panama City experiment. This discrepancy only underscores the need to understand this problem more completely.

Finally, an unnormalized self-coherent plot is shown in Figure 5. Each curve is calculated from the numerator of Equation (1) with the substitution n=m, which yields Equation (2):

$$\hat{\gamma}(t) = \left\langle Z_n(t) Z_m^*(t) \right\rangle \qquad (2)$$

This plot was made utilizing hydrophone 66 of Run 19 and Run 20. Again, the effect of the increased sea roughness is seen by the significant variation in the resulting functions between Run 19 and Run 20. The results shown in Figures 3 and 5 may be more easily understood utilizing Figure 6. When the scattered signal is first received at a given phone, the self-covariant response is merely a representation of the signals autocorrelation function. However, as time increases, scattering from larger ensonified surface areas can interfere destructively to create a sharper rate of decorrelation on the backside of the function's peak.

Conclusion

The vertical covariances measured in this experiment decrease more rapidly with receiver separation than those measured by Dahl and McConnell (1). An understanding of the source of these differences requires the development of a theory to predict the time varying coherence as a function of experimental geometry and environmental factors.

Acknowledgments

This research was supported by the Office of Naval Technology (Program Element 0602435N) and the High-Frequency Bottom Scattering Program at the Naval Research Laboratory (Program Element 0601153N) managed by Drs. Robert W. Farwell and Steve Stanic, respectively. NRL contribution number PP/7174-93-0034.

References

1. Dahl, P.H. and McConnell, S.O., Measurements of Acoustic Spatial Coherence in a Near-Shore Environment, August 1990, APL-UW TR9016, Applied Physics Laboratory, University of Washington, Seattle, WA.

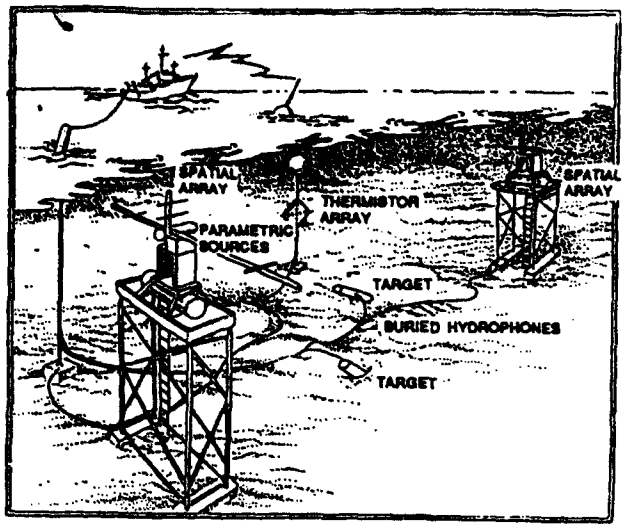

Figure 1. Experimental geometry.

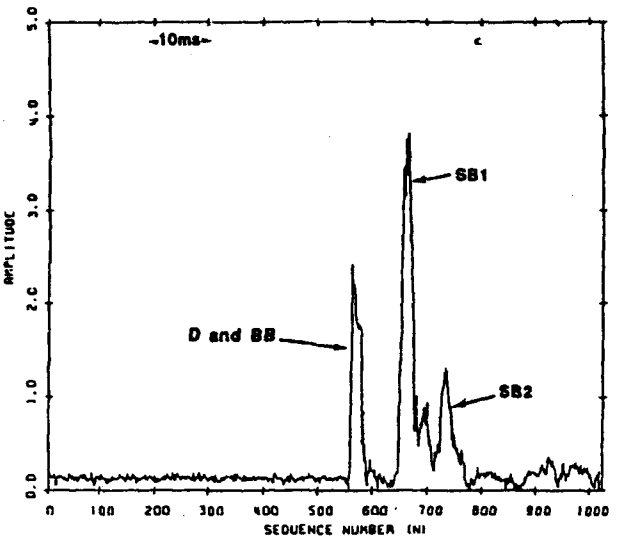

Figure 2. Event arrivals.

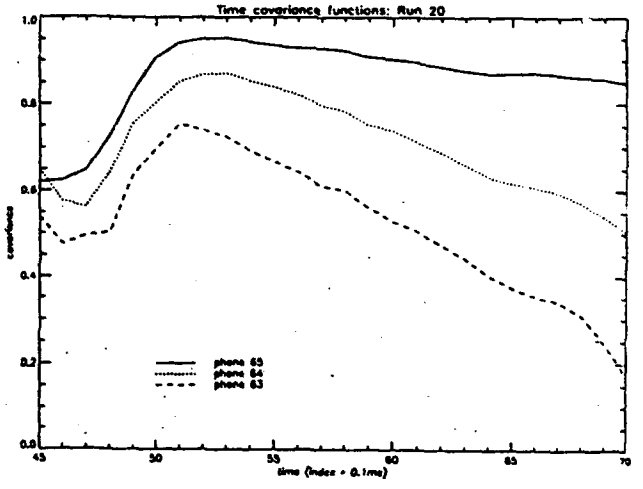

Figure 3. Time covariance functions.

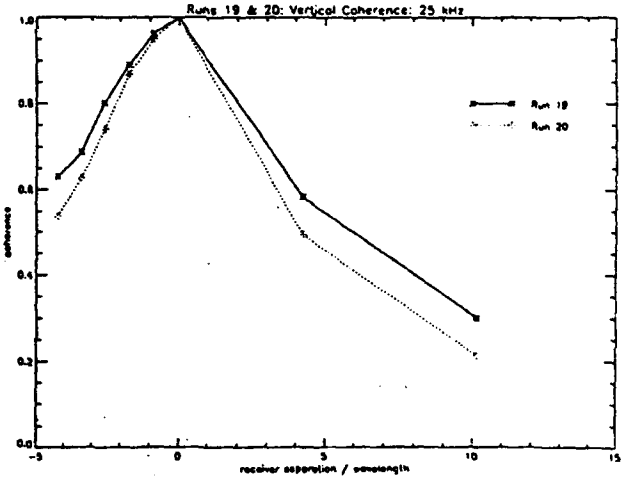

Figure 4. Vertical spatial coherence, runs 19 and 20.

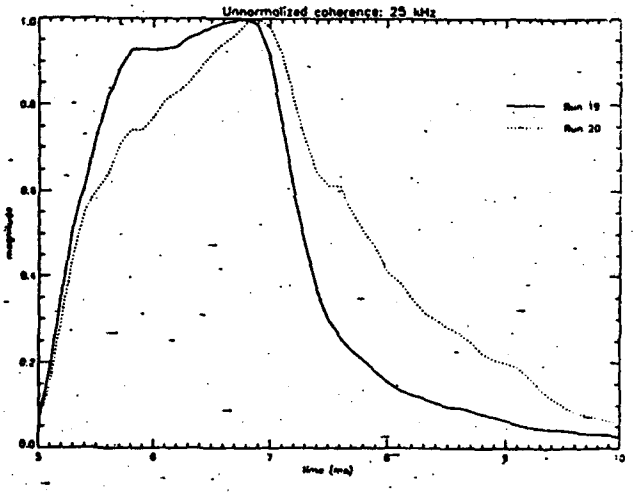

Figure 5. Unnormalized self-coherent plots, runs 19 and 20.

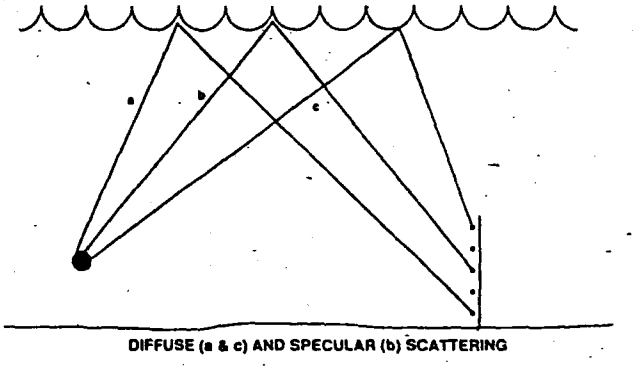

Figure 6. Scattering geometries.